

AIM: Adaptive Intra-Network Modulation for Balanced Multimodal Learning

Shu Shen , *Student Member, IEEE*, C. L. Philip Chen , *Life Fellow, IEEE*, and Tong Zhang

Abstract—Multimodal learning has significantly enhanced machine learning performance but still faces numerous challenges and limitations. Imbalanced multimodal learning is one of the problems extensively studied in recent works and is typically mitigated by modulating the learning of each modality. However, we find that these methods typically hinder the dominant modality’s learning to promote weaker modalities, which affects overall multimodal performance. We analyze the cause of this issue and highlight a commonly overlooked problem: optimization bias within networks. To address this, we propose Adaptive Intra-Network Modulation (AIM) to improve balanced modality learning. AIM accounts for differences in optimization state across parameters and depths within the network during modulation, achieving balanced multimodal learning without hindering either dominant or weak modalities for the first time. Specifically, AIM decouples the dominant modality’s under-optimized parameters into Auxiliary Blocks and encourages reliance on these performance-degraded blocks for joint training with weaker modalities. This approach effectively prevents suppression of weaker modalities while enabling targeted optimization of under-optimized parameters to improve the dominant modality. Additionally, AIM assesses modality imbalance level across network depths and adaptively adjusts modulation strength at each depth. Experimental results demonstrate that AIM outperforms state-of-the-art imbalanced modality learning methods across multiple benchmarks and exhibits strong generalizability across different backbones, fusion strategies, and optimizers.

Index Terms—Multimodal learning, Imbalanced multimodal learning, network optimization.

I. INTRODUCTION

HUMANS perceive and understand the surrounding world by integrating multiple senses, such as vision, hearing, and touch [1], [2]. Inspired by this, multimodal learning, which leverages and fuses data from diverse sensors, has attracted considerable attention and achieved substantial progress [3]–[7]. In recent years, it has significantly improved the performance of machine learning models in various applications, including action recognition [8], [9], emotion recognition [10], [11], and audio-visual speech recognition [12].

Despite rapid progress, multimodal learning still faces difficulties in effectively utilizing information and fully exploiting the potential of each modality. Recent studies have identified the “modality imbalance” problem as a key factor underlying these challenges [13]–[16]. This issue stems from differences in performance and convergence rates across modalities, resulting in uncoordinated convergence under a unified joint training objective [14], [16]. Consequently, weak modalities with poorer performance are suppressed by dominant ones with better performance during optimization, preventing them from being adequately exploited. To mitigate this effect,

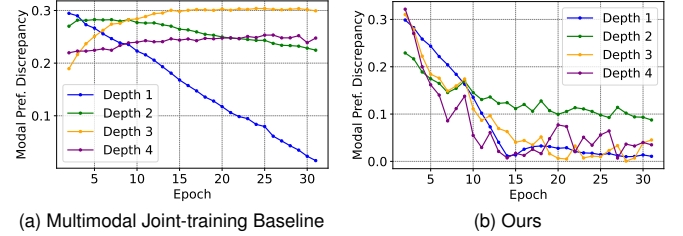


Fig. 1. The variation of modality performance discrepancy at different depths during training on the CREMA-D dataset in (a) the multimodal joint-training baseline and (b) our method.

various methods [14]–[19] have been proposed to modulate the learning processes of different modalities. By slowing the learning of dominant modalities, these approaches encourage the model to better learn from and exploit weaker modalities, thereby improving overall multimodal performance. However, these methods inevitably compromise the learning of dominant modalities, leaving room for further improvement in multimodal performance. How to enhance weaker modalities without hindering the learning of dominant ones remains an open challenge for balanced multimodal learning.

This paper analyzes the causes of this challenge from the perspective of a problem we term “intra-network optimization bias”. This problem refers to the phenomenon that different parameters and depths within a deep neural network exhibit varying optimization pace due to factors such as parameter initialization [20] and gradient instability [21], [22]. This phenomenon may give rise to two issues during the training of multimodal networks. On the one hand, each unimodal network contains parameters with varying optimization state, with some already well-optimized while others remain under-optimized. On the other hand, performance discrepancy across unimodal networks varies with network depth. However, existing balanced multimodal learning methods typically perform modulation at the granularity of an entire unimodal network, overlooking the issue of intra-network optimization bias. For example, Peng et al. [14] and Wei et al. [16] slow down the learning of the dominant modality by multiplying the gradients of all its network parameters by the same factor smaller than the weaker ones. Fan et al. [18] assign a smaller weight to the classification loss of the dominant unimodal network. Wei et al. [19] periodically reinitialize all parameters of the dominant unimodal network with greater intensity during training. Consequently, these methods share two key limitations. First, they slow the learning of under-optimized parameters within the dominant modality to the same extent

as well-optimized ones, which hampers its overall learning. Second, they do not account for the variation in multimodal imbalance levels across network depths arising from changes in cross-modal performance discrepancies, leading to limited modulation effectiveness. Therefore, we pose a critical question: *How to incorporate intra-network optimization bias into the design of modulation for balanced multimodal learning?*

To this end, we propose Addaptive Intra-Network Modulation (**AIM**), which enables balanced multimodal learning without suppressing either dominant or weak modalities. **AIM** employs a hierarchical intra-network modulation framework that adaptively adjusts the learning of different network parameters and depths during training, enhancing balanced multimodal performance. To support performance evaluation and loss computation for intra-network modulation, we propose depth-aware prototypes. They provide adaptive optimization objectives across depths, which are designed with the insight that different network depths possess distinct optimization capacities, with deeper layers typically yielding outputs closer to the ground truth. Within the hierarchical modulation framework, **AIM** first employs a modulator at each network depth to balance unimodal learning while accounting for the varying optimization states of network parameters. Then, it adaptively adjusts the modulation strength across depths based on the imbalance level among modalities to improve training effectiveness.

Specifically, the modulator at each depth employs a parameter decoupling mechanism that dynamically extracts under-optimized parameters from each modality's network to construct corresponding performance-degraded Auxiliary Blocks. An Auxiliary-Weak Interaction strategy is then applied, adaptively guiding the dominant modality to rely more on its Auxiliary Block instead of the full network (i.e., original unimodal network) for joint training with weaker modalities, producing a multimodal modulation loss. As a result, the performance-degraded Auxiliary Block of the dominant modality can effectively eliminate the suppression of the weaker modalities during joint training. Moreover, the dominant modality achieves targeted optimization of its under-optimized parameters through the Auxiliary Block, thereby facilitating its learning. Subsequently, **AIM** estimates imbalance levels at each depth via cross-modal performance discrepancies and uses them to weight and aggregate modulation losses, enabling depth-adaptive modulation.

The contributions of this paper can be summarized as:

- This work highlights a previously overlooked issue in balanced multimodal learning, termed intra-network optimization bias, and proposes an adaptive intra-network modulation (**AIM**) framework to improve multimodal performance. Experiments demonstrate that **AIM** generalizes well across different backbones and fusion strategies, outperforming existing balanced multimodal learning approaches on multiple benchmarks.
- **AIM** introduces a novel parameter decoupling mechanism to construct Auxiliary Blocks containing under-optimized parameters. Combined with an Auxiliary-Weak interaction mechanism, it enables the enhancement of

weak modality learning without hindering the dominant modality for the first time.

- **AIM** accounts for the variation in modality imbalance level caused by convergence biases across network depths. It designs a depth-adaptive modulation scheme to adjust modulation strength accordingly, thereby improving the efficiency of multimodal model learning.
- We specifically design depth-aware prototypes (**DAP**) for intra-network modulation in **AIM**. **DAP** accounts for varying optimization capacities across network depths and provides depth-adaptive objectives for performance evaluation and loss computation.

II. RELATED WORKS

A. Multimodal Learning

With the advancement of sensor technologies as well as data acquisition and processing techniques, large amounts of data from diverse sources, types, and formats have emerged, giving rise to multimodal learning [7], [23], [24]. By integrating the complementary information of different modalities, multimodal learning enables models to produce more accurate outputs and significantly improves the performance of various existing tasks. For example, in emotion recognition, Li et al. [25]–[28] significantly enriched emotional representations by leveraging modalities with limited emotional content to enhance those with richer emotional information. In action recognition, Kazakos et al. [8] designed a novel framework for multi-modal temporal binding that outperforms individual modalities. Gao et al. [9] leveraged audio as a preview to eliminate redundant visual information. In the task of audio-visual speech recognition [12], Hu et al. [29] improved recognition accuracy by effectively learning temporal joint representation among multiple modalities.

In recent years, an increasing number of studies have focused on the emerging challenges posed by real-world scenarios in multimodal learning [30]–[35]. Among these challenges, imbalanced multimodal learning has received considerable attention. It refers to a situation where the model fails to fully exploit all modalities under the widely adopted joint training paradigm [15], [17]. In this case, the learning of certain modalities may be suppressed by others, which ultimately undermines the overall performance of multimodal models. In this work, we propose Adaptive Intra-Network Modulation (**AIM**) to address the problem of imbalanced multimodal learning by modulating the learning processes of each unimodal.

B. Imbalanced Multimodal Learning

Multimodal models are expected to outperform their unimodal counterparts by leveraging cross-modality complementarity, typically through joint training under a unified objective. However, recent studies reveal that such strategies often fail to fully utilize each modality, sometimes resulting in performance inferior to unimodal baselines [15]. This issue is known as imbalanced multimodal learning. Several studies have empirically attributed this issue to the discrepancy between modalities, which results in different optimization and

convergence rates, making a shared objective suboptimal [15], [36]. Additionally, theoretical evidence has shown that joint training can only effectively capture information from a subset of modalities [13].

Building on these insights, various methods have been proposed to mitigate imbalance in multimodal learning. Early approaches introduced unimodal-specific losses [15] or leveraged knowledge distillation with pretrained encoders [37]. More recent works [14], [16], [18], [19] dynamically assess each unimodal's performance or optimization status and modulate its learning accordingly. For instance, Peng et al. [14] scale modality gradients by coefficients negatively correlated with performance, encouraging underperforming modalities while slowing dominant ones. Wei et al. [19] proposed a diagnosing and re-learning method that applies stronger reinitialization to better-optimized modalities. While effective, these methods often improve weaker modalities through the suppression of dominant ones, potentially degrading overall performance, and typically lack fine-grained modulation of learning within unimodal networks. To this end, we propose a method that enhances weaker modalities without suppressing dominant ones and enables differentiated modulation of learning across parameters and network depths within each unimodal network.

C. Intra-Network Optimization Bias In Deep Neural Networks

Deep neural networks leverage hierarchical structures to model complex relationships and achieve strong performance across various tasks [38], [39]. However, their deep architecture also makes training and optimization more complex. Numerous studies [20], [21], [40]–[42], [42], [43] have shown that parameters across different network depths exhibit distinct convergence behaviors, a phenomenon termed “intra-network optimization bias”. Some works analyze this bias from the perspective of gradient flow. Early studies identified the vanishing gradient problem [40], [41], where gradients diminish during backpropagation, which in turn suggests that layers may converge at different rates. A number of later works [42]–[44] intuitively leveraged the idea of layer-wise convergence differences to improve the training efficiency of deep neural networks. Recently, Chen et al. [21] introduced the phenomenon of Layer Convergence Bias, showing that the convergence speed of specific layers is not reliably positively correlated with their gradient magnitudes, and that shallow layers learn and converge faster than deeper ones. Beyond gradient analysis, numerous studies have investigated the impact of employing different initialization strategies across parameters or depths on network optimization. Saratchandran et al. [20] showed that using smaller-variance normal initialization for the final layer compared to other layers reduces overparameterization and improves optimization efficiency. Liu et al. [22] proposed a Chaotic Differential Evolution Grey Wolf algorithm to enable optimal initialization for different model parameters. In this work, we investigate the impact of Intra-Network Optimization Bias on imbalanced multimodal learning and propose a method based on parameter decoupling and depth-adaptive modulation to enhance multimodal learning performance.

D. Prototypical Method

A prototype refers to a representative feature vector of a given class, which can be interpreted as the class center. It is typically computed as the average of the feature embeddings for all samples in a given class, effectively serving as the centroid in the embedding space. Prototypes have been widely adopted in few-shot and zero-shot learning [45]–[48] as well as in classification tasks where samples are labeled according to the nearest class prototype in the embedding space. In recent years, prototype-based methods have also been extended to address challenges in out-of-distribution (OOD) detection [49], long-tailed recognition [50], domain adaptation [51], [52], and unsupervised learning [53]. As a non-parametric classifier [45], [53], the prototype offers a modeling paradigm characterized by greater stability, lower complexity, and enhanced interpretability.

In this work, we propose a novel prototypical method, termed Position-Aware Prototypes (PAP), which provides an adaptive mechanism for estimating the optimization status across different network depths. Unlike existing methods that compute prototypes directly from labeled sample embeddings, our approach starts from the class set and derives prototypes through backward optimization at varying network depths.

III. PROPOSED APPROACH

A. Multimodal Framework

The proposed Adaptive Intra-Network Modulation (**AIM**) focuses on the joint-training multimodal framework illustrated in Fig. 2(a), following previous works [14], [16], [18], [19]. Consider a multimodal dataset consisting of N samples $\{x_1, \dots, x_N\}$ from K classes, each sample $x_i = \{x_i^1, \dots, x_i^M\}$ with label y_i comprises data from M modalities. The framework processes each sample x_i through modality-specific encoders $\{\mathbf{E}^m\}_{m=1}^M$ to extract unimodal feature representations. These features are then integrated via a fusion strategy $\Theta_{\mathcal{F}}$, yielding a combined multimodal feature that is subsequently passed to a classifier $\Theta_{\mathcal{C}}$ to generate the predicted label \hat{y}_i . The calculation of the multimodal framework $\Theta_{\mathcal{M}}(\cdot)$ can be formulated as follows:

$$\hat{y}_i = \Theta_{\mathcal{M}}(x_i) = \Theta_{\mathcal{C}}(\Theta_{\mathcal{F}}(\mathbf{E}^1(x_i^1), \dots, \mathbf{E}^M(x_i^M))). \quad (1)$$

Our proposed **AIM** is agnostic to the choice of encoder backbones and fusion strategies. Experimental results presented in Sec. IV-D demonstrate its effectiveness across different backbone architectures and fusion methods.

B. Overview of Adaptive Intra-Network Modulation (AIM)

We propose Adaptive Intra-Network Modulation (**AIM**) to address the issue of imbalanced multimodal learning inherent in the framework described in Sec. III-A. **AIM** adaptively modulates the learning progress across different parameters and depths within each unimodal encoder, promoting more balanced learning across modalities. As illustrated in Fig. 2(b), **AIM** first partitions each encoder \mathbf{E}^m corresponding to modality m into D sequential blocks from shallow to deep, denoted as $\{\mathbf{E}_d^m\}_{d=1}^D$, where one block may contain one or

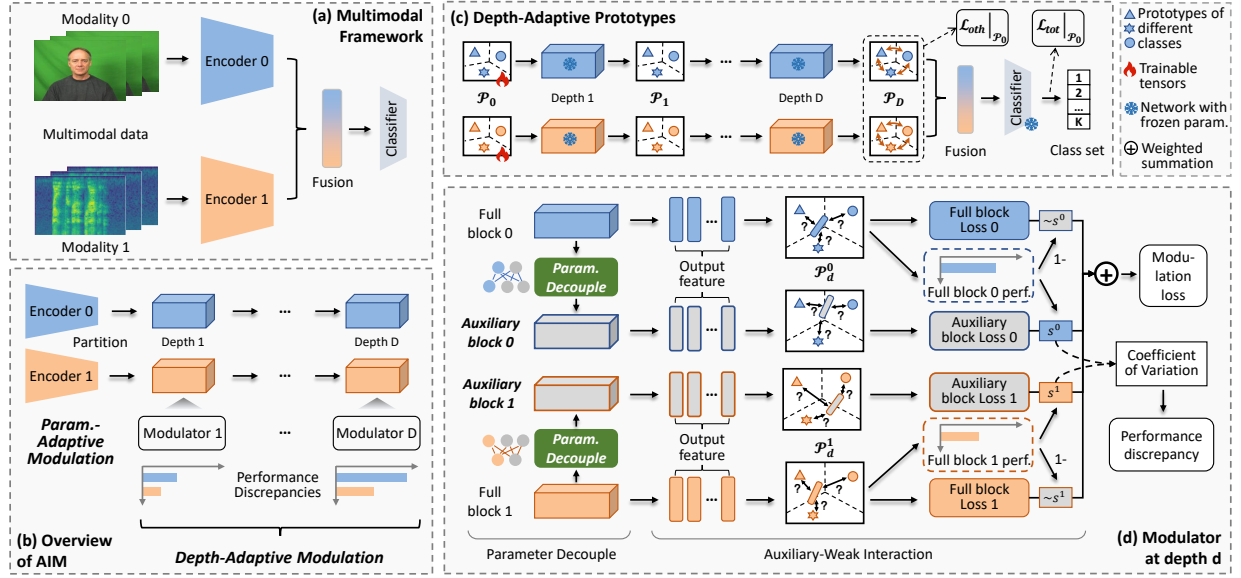


Fig. 2. An overview of the proposed Adaptive Intra-Network Modulation (AIM). (a) The multimodal framework; (b) Overview of the hierarchical architecture of AIM. AIM partitions each unimodal backbone from shallow to deep into D blocks and employs a modulator \mathbf{M}_d at each depth d ; (c) Detailed implementation of the modulator \mathbf{M}_d at depth d . Without loss of generality, this figure illustrates the case of two modalities, with blue and yellow representing different modalities. The detailed implementation of the parameter-decoupling mechanism in each modulator is presented in Fig. 3.

more network layers. Taking the ResNet18 backbone as an example, each of its four residual stages is treated as one block in this work. Subsequently, AIM employs a hierarchical modulation scheme that first applies a modulator \mathbf{M}_d to all modality-specific blocks at depth d , denoted as $\{\mathbf{E}_d^m\}_{m=1}^M$. \mathbf{M}_d decouples under-optimized parameters from each modality-specific block and adaptively modulates their learning across modalities, producing a multimodal modulation loss \mathcal{L}_d and an imbalance level estimation α_d at depth d . $\{\mathcal{L}_d\}_{d=1}^D$ are then aggregated according to $\{\alpha_d\}_{d=1}^D$ to produce the overall modulation loss \mathcal{L}_{mod} , enabling imbalance-adaptive modulation across depths for more balanced multimodal learning.

The following sections are organized as follows. Sec. III-C introduces the depth-adaptive prototypes, which serve as the foundation for the overall modulation. Sec. III-D describes the implementation of each cross-modal parameter modulator \mathbf{M}_d . Sec. III-E details how AIM aggregates $\{\mathcal{L}_d\}_{d=1}^D$ from all modulators to modulate learning across depths. Sec. III-F summarizes the training and inference procedure of the multimodal framework integrating AIM.

C. Depth-Adaptive Prototypes

To enable modulation of parameter learning across depths, AIM requires dynamic computation and evaluation of loss and optimization status at each depth during training. Previous works [14], [16], [18], [19] typically use ground-truth labels to compute losses and assess model optimization status, regarding the labels as the optimal objective. While this strategy can be adopted by AIM, using ground-truth labels as a unified optimization objective across depths overlooks the varying optimization capacities of different depths. That is, deeper networks often produce outputs closer to the ground truth, exhibiting higher optimization capacities than shallower ones.

To this end, AIM introduces Depth-Adaptive Prototypes (DAP) for loss computation and optimization status evaluation at different depths of a network during training. At each depth, DAP introduces a set of feature vectors (i.e., prototypes), whose number corresponds to the total number of classes. Each prototype has the same dimensionality as the model representation at that depth and serves as the optimal latent feature that, when propagated forward, leads to the prediction of the corresponding class under the current model state. Specifically, in the multimodal framework defined in Sec. III-A, we set a group of prototypes at each depth d of the encoder \mathbf{E}^m for each modality m , denoted as $\mathcal{P}_d^m = \{(p_d^m)_k\}_{k=1}^K$, where K is the number of class. To obtain all prototypes in the framework, we first pre-train the multimodal framework and freeze all its parameters. Then, we randomly initialize a set of learnable tensors $\tilde{\mathcal{P}}_0 = \{\tilde{\mathcal{P}}_0^m\}_{m=1}^M$, compute their outputs through the whole multimodal framework, and calculate the loss with the class set \mathcal{Y} , as shown in Eq. (2).

$$\mathcal{L}_{\text{tot}}|_{\tilde{\mathcal{P}}_0} = CE(\Theta_{\mathcal{M}}(\tilde{\mathcal{P}}_0), \mathcal{Y}). \quad (2)$$

$CE(\cdot, \cdot)$ is the cross-entropy loss, $\Theta_{\mathcal{M}}(\cdot)$ is the calculation of the multimodal framework defined in Eq. (1). $\mathcal{Y} = [0, \dots, K-1]$ is the class set of the dataset, which is a K -dimensional vector of integers and is different from the sample's ground-truth label. Through the forward propagation of $\tilde{\mathcal{P}}_0$, prototypes at different depths, $\tilde{\mathcal{P}}_1, \dots, \tilde{\mathcal{P}}_D$, can be computed as defined in Eq. (3).

$$\tilde{\mathcal{P}}_d^m = \mathbf{E}_{\sim d}^m(\tilde{\mathcal{P}}_0^m), \quad \forall m \in [1, M], \forall d \in [1, D], \quad (3)$$

where $\mathbf{E}_{\sim d}^m$ denotes the sub-network composed of the first d blocks of the encoder \mathbf{E}^m for modality m . To further constrain the optimization of $\tilde{\mathcal{P}}_0$, we encourage the prototypes of different classes in the deepest block, $\tilde{\mathcal{P}}_D$, obtained through

the forward propagation of $\tilde{\mathcal{P}}_0$, to be as mutually orthogonal as possible, leading to the loss term defined in Eq. (4).

$$\mathcal{L}_{oth}|\tilde{\mathcal{P}}_0 = \frac{1}{M} \sum_{m=1}^M \|\langle S(\tilde{\mathcal{P}}_D^m), S(\tilde{\mathcal{P}}_D^m)^T \rangle - I_{K \times K}\|_F \quad (4)$$

$\tilde{\mathcal{P}}_D$ can be computed via Eq. (3) using $\tilde{\mathcal{P}}_0$. $\langle \cdot, \cdot \rangle$ denotes the cosine similarity between two tensors. $S(\cdot)$ stacks all tensors in a set into a single tensor. The superscript T indicates matrix transposition. $I_{K \times K} \in \mathbb{R}^{K \times K}$ is the identity matrix. $\|\cdot\|_F$ denotes the Frobenius norm. Thus, $\tilde{\mathcal{P}}_0$ can be optimized via Eq. (5):

$$\mathcal{P}_0 = \arg \min_{\tilde{\mathcal{P}}_0} \mathcal{L}_{tot}|\tilde{\mathcal{P}}_0 + \mathcal{L}_{oth}|\tilde{\mathcal{P}}_0. \quad (5)$$

\mathcal{P}_0 represents the optimized $\tilde{\mathcal{P}}_0$. The prototypes at each depth d in the encoder \mathbf{E}^m for modality m , denoted as \mathcal{P}_d^m , are then obtained by replacing $\tilde{\mathcal{P}}_0$ with \mathcal{P}_0 in Eq. (3). Since forward propagation $\mathbf{E}_{\sim d}^m$ differs for different depths d , the prototypes obtained across depths varies accordingly. Thus, they can adapt to the representation and optimization capacity of each depth and provide depth-wise objectives for loss computation and optimization status evaluation.

D. Cross-Modal Parameter-Adaptive Modulation

In the Modulator \mathbf{M}_d at depth d , we first introduce a **parameter decoupling mechanism** that separates under-optimized parameters from each modality-specific network block at depth d , forming new network blocks. The original block is referred to as the “full block”, while the newly formed one is termed the “pseudo-weak block” for that modality, as it aggregates under-optimized parameters and exhibits weaker performance than the full block. Subsequently, we design a **weak-pseudo-weak interaction strategy**, encouraging the dominant modality to favor its pseudo-weak block over the full block for joint training with the full blocks of weaker modalities. On one hand, replacing the full block of the dominant modality with its lower-performing pseudo-weak block helps alleviate suppression of weaker modalities during joint training. On the other hand, optimizing the pseudo-weak block during joint training simultaneously updates the corresponding full block, ensuring adequate learning for the dominant modality. This enables a balanced multimodal learning process where neither strong nor weak modalities are suppressed.

1) **Parameter-Decoupling Mechanism**: The implementation of parameter-decoupling mechanism is illustrated in Fig. 3. For the network block at depth d of modality m encoder, denoted as \mathbf{E}_d^m , its parameters θ are first flattened layer by layer. Then, the flattened parameters are mapped into the latent parameter space by encoder Φ_{lat} to obtain θ_{lat} : $\theta_{lat} = \Phi_{lat}(\theta)$. Based on θ_{lat} , the encoder Φ_{mask} learns a mask w of the same dimension: $w = \Phi_{mask}(\theta_{lat})$. The mask and its complement are applied to θ_{lat} via element-wise multiplication, producing θ_{lat}^{op} and θ_{lat}^{uop} :

$$\theta_{lat}^{op} = \theta_{lat} \odot w, \quad \theta_{lat}^{uop} = \theta_{lat} \odot (1 - w). \quad (6)$$

\odot is the element-wise multiplication. θ_{lat}^{op} and θ_{lat}^{uop} are then decoded by Ψ back into the parameter space, yielding θ^{op}

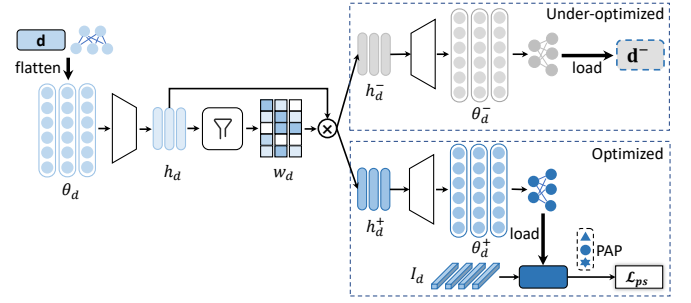


Fig. 3. The detailed implementation of the parameter-decoupling mechanism.

and θ^{uop} : $\theta^{op} = \Psi(\theta_{lat}^{op})$, $\theta^{uop} = \Psi(\theta_{lat}^{uop})$. θ^{op} and θ^{uop} are decoupled well-optimized and under-optimized parameters from the original network block with parameter θ . They are finally loaded into the network structure identical to \mathbf{E}_d^m , resulting in two output network blocks, $\mathbf{E}_d^{m,op}$ and $\mathbf{E}_d^{m,uop}$, respectively. The encoders and decoders in the parameter-decoupling mechanism are effectively trained by minimizing the loss \mathcal{L}_{pdm} defined in Eq. (7).

$$\mathcal{L}_{pdm} = \frac{1}{|I_d^m|} \sum_{i=1}^{|I_d^m|} \delta[\mathbf{E}_d^{m,op}(I_d^m), (p_d^m)_{y_i}]. \quad (7)$$

I_d^m represents the set of input feature vectors of network block \mathbf{E}_d^m , i.e., the output of \mathbf{E}_{d-1}^m and equals to x^m when $d = 0$. $|\cdot|$ denotes the cardinality of set I_d^m . $I_{d,i}^m$ represents the feature vector indexed by i , and y_i is its corresponding ground-truth label. $\delta[\cdot, \cdot]$ denotes the Euclidean distance between two vectors. $(p_d^m)_{y_i}$ denotes the **DAP** for class y_i of modality m at depth d . Minimizing \mathcal{L}_{pdm} encourages the output of $\mathbf{E}_d^{m,op}$ to align with the **DAP**, such that the parameters θ^{op} selected by the mask w are well-optimized with high performance, while the remaining parameters θ^{uop} are under-optimized.

For the network block \mathbf{E}_d^m at each depth d in the encoder of each modality m , **AIM** applies the parameter decoupling mechanism to obtain $\mathbf{E}_d^{m,op}$ and $\mathbf{E}_d^{m,uop}$. The block $\mathbf{E}_d^{m,uop}$ with under-optimized parameters is referred to as the **Pseudo-Weak Block** corresponding to the full block \mathbf{E}_d^m of modality m . For clarity, it is denoted as $\tilde{\mathbf{E}}_d^m$ in the following sections.

2) **Weak-Pseudo Weak Interaction Strategy**: The weak pseudo-weak interaction strategy enables dominant modalities to interact with weak modalities using their performance-degraded pseudo-weak blocks during multimodal joint training. In this process, the performance of the full blocks \mathbf{E}_d^m of each modality m at depth d is first evaluated utilizing **DAP**:

$$s_d^m = \mathbb{E}_{\mathbf{p}(I_d^m, y)} \left[\frac{\exp(-\delta[\mathbf{E}_d^m(I_d^m), (p_d^m)_y])}{\sum_{y'} \exp(-\delta[\mathbf{E}_d^m(I_d^m), (p_d^m)_{y'}])} \right]. \quad (8)$$

s_d^m is the performance of the full block \mathbf{E}_d^m . Then, the loss of full block \mathbf{E}_d^m and pseudo-weak block $\tilde{\mathbf{E}}_d^m$ of each modality

m at depth d are calculated, formulated in Eq. (9).

$$\begin{aligned}\mathcal{L}_d^m &= \frac{1}{|I_d^m|} \sum_{i=1}^{|I_d^m|} \delta [\mathbf{E}_d^m(I_{d,i}^m), (p_d^m)_{y_i}], \\ \tilde{\mathcal{L}}_d^m &= \frac{1}{|\tilde{I}_d^m|} \sum_{i=1}^{|\tilde{I}_d^m|} \delta [\tilde{\mathbf{E}}_d^m(I_{d,i}^m), (p_d^m)_{y_i}],\end{aligned}\quad (9)$$

where \mathcal{L}_d^m and $\tilde{\mathcal{L}}_d^m$ represent the loss of \mathbf{E}_d^m and $\tilde{\mathbf{E}}_d^m$. Subsequently, $\{\mathcal{L}_d^m\}_{m=1}^M$ and $\{\tilde{\mathcal{L}}_d^m\}_{m=1}^M$ are integrated based on $\{s_d^m\}_{m=1}^M$, which can be formulated as follows:

$$\mathcal{L}_d = \sum_{m=1}^M \left[(1 - s_d^m) \mathcal{L}_d^m + s_d^m \tilde{\mathcal{L}}_d^m \right], \quad (10)$$

where

$$s_d^m = \frac{\exp(s_d^m)}{\sum_{j=1}^M \exp(s_d^j)}. \quad (11)$$

\mathcal{L}_d is the multimodal modulation loss obtained from modulator \mathbf{M}_d at depth d of the multimodal framework. The more dominant modalities with higher performance s_d^m have a lower weight of the loss of their full blocks and a higher weight of their pseudo-weak blocks during joint training, and vice versa for weaker modalities. With the parameters in $\mathbf{E}_d^{m,op}$ of dominant modalities fixed, updates to their pseudo-weak blocks during joint training simultaneously optimize the corresponding full blocks, ensuring sufficient learning of the dominant modalities themselves. Moreover, since the pseudo-weak blocks of dominant modalities are performance-degraded, they substantially mitigate the suppression imposed on weak modalities.

E. Depth-Adaptive Modulation

The modulator \mathbf{M}_d derives the multimodal modulation loss \mathcal{L}_d , which balances the learning across modalities at depth d , as detailed in Sec. III-D. However, as discussed in Sec. I, different depths in deep networks exhibit varying convergence rates, leading to varying levels of imbalance between modalities at different depths. Therefore, we propose adaptively integrating multimodal modulation losses across depths based on their imbalance levels, applying stronger modulation to depths with higher imbalance. Specifically, at each depth d , we compute the performance discrepancy between modalities to evaluate the level of imbalance across modalities. Considering that performance values may vary substantially across depths, we employ the Coefficient of Variation [54] to calculate the discrepancy, which is formulated in Eq. (12).

$$\alpha_d = \frac{\sqrt{\frac{1}{M} \sum_{m=1}^M (s_d^m - \bar{s}_d)^2}}{\bar{s}_d}, \quad (12)$$

where s_d^m is calculated from Eq. (8). $\bar{s}_d = \frac{1}{M} \sum_{m=1}^M s_d^m$. α_d is the performance discrepancy between modalities that measures the imbalance level in depth d . Subsequently, the multimodal modulation losses $\{\mathcal{L}_d\}_{d=1}^D$ at different depths are weighted

by $\{\alpha_d\}_{d=1}^D$ and integrated to form the total modulation loss of **AIM**, as formulated in Eq. (13).

$$\mathcal{L}_{mod} = \sum_{d=1}^D \alpha_d \cdot \mathcal{L}_d. \quad (13)$$

F. Training and Inference

During training, we first jointly train the depth-adaptive prototypes and parameter decoupling mechanism of **AIM** together with the multimodal framework for E epochs. After that, the complete **AIM** is employed to modulate the training of the multimodal framework. The value of E will be analyzed in Sec. IV-I. During testing, the well-trained multimodal framework is directly used for prediction.

IV. EXPERIMENTS

In this section, the effectiveness of the proposed Adaptive Intra-Network Modulation (**AIM**) is evaluated compared with 8 state-of-the-art methods for balanced multimodal learning on several benchmarks. In the following section, we will first introduce the experimental settings in Sec. IV-A. Then, the comparison with the baselines and ablation study will be presented respectively in Sec. IV-B and IV-C. In the subsequent sections, we also provide detailed discussions on multiple aspects, including the generalizability of the **AIM** and the roles of its components.

A. Experimental Setups

1) *Datasets*: Experiments are conducted on four commonly used multimodal datasets in previous methods [14], [16], [18], [19], covering different modality combinations and tasks. (1) **CREMA-D** [55] is an emotion recognition dataset comprising audio and visual modalities. It contains 7,442 clips from 91 actors, each lasting 2–3 seconds, where the actors spoke from a selection of 12 predefined sentences. The clips cover six emotion categories: angry, happy, sad, neutral, disgust, and fear. The dataset is randomly split into a training set with 6,698 samples and a test set with 744 samples. (2) **Kinetics-Sounds (KS)** [56] is a subset of the Kinetics dataset [57], which consists of YouTube videos covering 400 human action categories such as air drumming, catching fish, and driving car. KS includes 31 selected categories from Kinetics with two modalities, audio and visual. These videos were manually annotated via Mechanical Turk and cropped to 10-second segments centered around the action. The dataset contains 19k video clips in total, with 15k for training, 1.9k for validation, and 1.9k for testing. The 31 selected categories in KS are those potentially manifested both visually and aurally, such as musical instrument performances (e.g., guitar, violin) and tool usage (e.g., lawn mowing, shoveling snow), among others. (3) **UCF-101** [58] is an action recognition dataset comprising two modalities: RGB and optical flow. It includes 101 human action categories, such as biking, diving, and horse riding. Following the original setting, the dataset is split into a training set with 9,537 samples and a test set with 3,783 samples. (4) **CMU-MOSI** [59] is a sentiment analysis dataset comprising

TABLE I

COMPARISON WITH METHODS FOR BALANCED MULTIMODAL LEARNING ON THE CREMA-D, KINETICS SOUNDS, AND UCF-101 DATASETS. BOLD AND UNDERLINE REPRESENT THE BEST AND SECOND BEST, RESPECTIVELY. JOINT-TRAINING WITH CONCATENATION FUSION IS USED AS A BASELINE FOLLOWING PREVIOUS WORKS.

| Method | CREMA-D (Audio+Visual) | | Kinetics-Sounds (Audio+Visual) | | UCF-101 (RGB+Optical Flow) | |
|-----------------|---------------------------|--------------|-----------------------------------|--------------|-------------------------------|--------------|
| | ACC | Macro-F1 | ACC | Macro-F1 | ACC | Macro-F1 |
| Joint-training | 67.47 | 67.80 | 65.04 | 65.12 | 67.34 | 66.93 |
| G-Blending [15] | 69.89 | 70.41 | 68.60 | 68.64 | 72.15 | 71.31 |
| OGM-GE [14] | 68.95 | 69.39 | 67.15 | 66.93 | 71.84 | 70.74 |
| Greedy [17] | 68.37 | 68.46 | 65.72 | 65.80 | 70.61 | 70.46 |
| PMR [18] | 68.55 | 68.99 | 65.62 | 65.36 | 72.25 | 71.16 |
| AGM [60] | 70.16 | 70.67 | 66.50 | 66.49 | 72.31 | 71.52 |
| MLA [33] | <u>79.70</u> | <u>79.94</u> | <u>71.32</u> | <u>71.23</u> | <u>74.51</u> | <u>73.44</u> |
| D&R [19] | 75.13 | 76.00 | 69.10 | 69.39 | 73.12 | 71.45 |
| OPM&OGM [16] | 75.10 | 75.91 | 68.00 | 68.12 | 72.36 | 71.62 |
| Ours | 81.32 | 82.00 | 72.40 | 72.27 | 77.43 | 78.12 |

3,228 YouTube videos, each containing audio, visual, and textual modalities. These videos are collected from 1,000 distinct speakers, covering 250 topics, and are segmented into 23,453 annotated clips.

2) *Compared methods*: To evaluate the effectiveness of the proposed Adaptive Intra-Network Modulation (**AIM**) in addressing the problem of imbalanced multimodal learning, several recent studies are introduced for comparison, including Gradient-Blending (**G-Blending**) [15], On-the-fly Gradient Modulation with Generalization Enhancement (**OGM-GE**) [14], **Greedy** [17], Prototypical Modality Rebalance (**PMR**) [18], Adaptive Gradient Modulation (**AGM**) [60], Multimodal Learning with Alternating Unimodal Adaptation (**MLA**) [33], Diagnosing and Re-learning (**D&R**) [19], and On-the-fly Prediction Modulation and On-the-fly Gradient Modulation (**OPM&OGM**) [16]. Joint training using concatenation fusion is adopted as the baseline for studying the imbalanced multimodal learning problem, following previous works [14], [16], [18], [19].

3) *Evaluation metrics*: In the experiments, accuracy (ACC) and macro-averaged F1 score (MacroF1) are employed to evaluate the performance of different methods following previous works [14], [16], [18], [19].

4) *Implementation Details*: The proposed method is built upon the multimodal framework described in Sec. III-A. Following previous works [14], [19], ResNet18 is adopted as the backbone for CREMA-D and Kinetic Sounds, and the models are trained from scratch. For UCF-101, ResNet18 is also used as the backbone and is pretrained on ImageNet. For CMU-MOSI, a transformer-based network serves as the backbone, with models trained from scratch. In the parameter decoupling module, both the encoder and decoder consist of a single fully connected layer. The encoder takes as input the number of parameters at each network layer and maps them to a 512-dimensional latent space. The decoder takes a 512-dimensional vector as input and outputs the same number of parameters as in the corresponding network layer. Dataset preprocessing follows previous works [14], [19]. All models are trained using SGD with a momentum of 0.9 and a learning rate of 1e-3, and all experiments are conducted on one NVIDIA RTX A6000.

B. Comparison With Baselines

Following previous works, we compare the classification performance of different methods across multiple multimodal datasets involving various tasks with different modality types. The results are presented in Table I.

1) *Comparison with the Joint-Training Baseline*: As shown in Table I, all methods for balanced multimodal learning, including ours, outperform the joint-training baseline across all datasets. Our method achieves particularly notable gains. On CREMA-D, it improves ACC and Macro-F1 by 13.85% and 14.20%, respectively, while on Kinetics-Sounds, the improvements are 7.36% and 7.15%. On UCF-101, we achieve 10.09% higher ACC and 11.19% higher Macro-F1 compared with joint training. These results confirm the presence of the imbalanced multimodal learning problem and underscore the importance of modulating each unimodal learning to achieve balanced multimodal learning.

2) *Comparison with State-of-the-Art Methods for Balanced Multimodal Learning*: Compared with recent studies on balanced multimodal learning, our method consistently achieves superior performance across all datasets. On the CREMA-D dataset, it outperforms the state-of-the-art method **MLA** by 1.62% in ACC and 2.06% in Macro-F1, and exceeds other advanced approaches such as **D&R** by at least 6.13% and 6%, respectively. On the Kinetics-Sounds dataset, our method yields at least a 3.3% gain in ACC over leading methods. On the UCF-101 dataset, our method shows improvements of 2.92% in ACC and 4.68% in Macro-F1 relative to **MLA**. This performance gain may be attributed to our modulation strategy that accounts for optimization-state variations across parameters and depths within the network and adaptively adjusts to them, leading to superior multimodal performance over existing methods.

C. Ablation study

Ablation studies are conducted to investigate the necessity of intra-network adaptivity in modulation provided by **AIM**. Specifically, the hierarchical modulation framework of **AIM** incorporates two forms of adaptivity: (1) in the modulator

TABLE II
ABLATION STUDY VALIDATING THE EFFECTIVENESS OF INTRA-NETWORK PARAMETER-ADAPTIVE MODULATION (**PA**) AND DEPTH-ADAPTIVE MODULATION (**DA**) IN **AIM**.

| Method | CREMA-D (Audio+Visual) | | Kinetics-Sounds (Audio+Visual) | | UCF-101 (RGB+Optical Flow) | |
|----------------|---------------------------|--------------|-----------------------------------|--------------|-------------------------------|--------------|
| | ACC | Macro-F1 | ACC | Macro-F1 | ACC | Macro-F1 |
| Joint-training | 67.47 | 67.80 | 65.04 | 65.12 | 67.34 | 66.93 |
| w/o PA | 75.12 | 75.41 | 68.83 | 68.36 | 71.43 | 71.39 |
| w/o DA | 80.14 | 80.52 | 71.82 | 71.51 | 75.92 | 75.52 |
| AIM | 81.32 | 82.00 | 72.40 | 72.27 | 77.43 | 78.12 |

at each depth, **AIM** adaptively decouples and optimizes the under-optimized parameters of dominant modalities; and (2) **AIM** adaptively adjusts the modulation strength across depths according to the multimodal imbalance level. To verify their effectiveness, we introduce two degraded variants, “w/o AP” and “w/o AD”. The “w/o AP” variant removes the parameter-decoupling module and auxiliary block from each modulator, directly computing the multimodal modulation loss \mathcal{L}_d as the performance-weighted sum of the full-block losses from the dominant and weak modalities. The “w/o AD” variant sets all depth-wise weights α_d in Eq. (13) to 1.

Table II presents a comparison between the two ablated variants, “w/o AP” and “w/o AD”, and the full **AIM** model. The results demonstrate that both ablations improve performance over the joint training baseline across multiple datasets, as both retain modulation of learning across different modalities. However, their performance is inferior to that of the complete **AIM** model, indicating that both forms of adaptivity are crucial for enhancing balanced multimodal learning. Furthermore, compared to “w/o AD”, the removal of parameter adaptivity (“w/o AP”) results in a larger performance decline relative to **AIM** and achieves a smaller gain over joint training. This suggests that parameter adaptivity within the modulation framework plays a more pivotal role in improving multimodal performance than depth adaptivity. The primary reason is that parameter adaptivity facilitates targeted learning of under-optimized parameters in dominant modalities, enabling balanced multimodal learning without hindering either dominant or weak modalities. Depth adaptivity, meanwhile, further refines the modulation effect beyond this foundation.

D. Validation of Generalizability

1) *Comparison Under Different Fusion Strategies*: To evaluate the effectiveness of the proposed **AIM** under different fusion strategies, we incorporate four commonly used fusion methods, namely Concatenation [61], Summation, FiLM [62], and Gated fusion [63], into our experiments, following previous works [14], [16], [18]. Concatenation fusion stacks feature vectors from all modalities before classification, whereas summation fusion adds them element-wise. FiLM and Gated fusion represent more advanced strategies that allow richer cross-modal interactions. Table III reports the performance of joint training baselines with different fusion strategies and their **AIM**-enhanced counterparts, along with unimodal results (audio-only and visual-only). The results reveal clear performance disparities between modalities, indicating the presence

TABLE III
PERFORMANCE ON CREMA-D AND KINETICS-SOUNDS DATASETS USING DIFFERENT FUSION METHODS. † INDICATES THE PROPOSED **AIM** IS APPLIED.

| Method | CREMA-D | | Kinetics-Sounds | |
|----------------|--------------|--------------|-----------------|--------------|
| | ACC | Macro-F1 | ACC | Macro-F1 |
| Audio-only | 63.17 | 63.11 | 60.44 | 60.25 |
| Visual-only | 68.15 | 68.28 | 37.78 | 37.23 |
| Concatenation | 71.37 | 71.47 | 62.39 | 61.95 |
| Summation | 68.68 | 67.86 | 59.51 | 60.42 |
| FiLM | 71.51 | 71.60 | 62.15 | 62.54 |
| Gated | 71.24 | 71.54 | 60.89 | 61.40 |
| Concatenation† | 81.32 | 82.00 | 72.40 | 72.27 |
| Summation† | 79.17 | 79.41 | 72.81 | 72.71 |
| FiLM† | 80.51 | 80.97 | 73.60 | 73.53 |
| Gated† | 79.36 | 79.57 | 71.96 | 71.95 |

TABLE IV
PERFORMANCE ON CREMA-D AND KINETICS-SOUNDS DATASETS WITH DIFFERENT OPTIMIZERS. † INDICATES THE PROPOSED **AIM** IS APPLIED.

| Optimizer | CREMA-D | | Kinetics-Sounds | |
|-----------|--------------|--------------|-----------------|--------------|
| | ACC | Macro-F1 | ACC | Macro-F1 |
| SGD | 71.37 | 71.47 | 62.39 | 61.95 |
| Adam | 64.92 | 64.03 | 62.36 | 62.40 |
| AdaGrad | 67.47 | 66.66 | 60.06 | 60.69 |
| SGD† | 81.32 | 82.00 | 72.40 | 72.27 |
| Adam† | 81.64 | 82.50 | 71.30 | 71.48 |
| AdaGrad† | 80.49 | 80.72 | 74.12 | 74.07 |

of modality imbalance. For instance, audio-only outperforms visual-only on the Kinetics-Sounds dataset. Moreover, certain fusion strategies under joint training even underperform unimodal methods. For example, summation fusion on Kinetics-Sounds yields lower accuracy than audio-only, suggesting that modality imbalance can suppress multimodal performance. In contrast, applying **AIM** consistently boosts performance across all fusion strategies and surpasses the performance of each unimodal, highlighting its effectiveness in mitigating modality imbalance across different fusion strategies.

2) *Comparison Using Different Optimizers*: To evaluate the effectiveness of the proposed **AIM** across different optimizers, in addition to SGD, two widely used optimizers, namely Adam [64] and AdaGrad [65], are also introduced to train the models. The results in Table IV show that incorporating **AIM** with joint training baseline consistently yields substantial performance

TABLE V
COMPARISON OF DIFFERENT METHODS USING A TRANSFORMER-BASED BACKBONE ON THE CMU-MOSI DATASET. METHODS THAT DO NOT SUPPORT MORE THAN TWO MODALITIES ARE EXCLUDED FROM THE COMPARISON.

| Method | CMU-MOSI (Audio+Visual+Text) | |
|-----------------|---------------------------------|--------------|
| | ACC | Macro-F1 |
| Joint-training | 76.96 | 75.68 |
| G-Blending [15] | 77.26 | 76.27 |
| AGM [60] | 77.26 | 76.02 |
| MLA [33] | <u>78.42</u> | <u>78.21</u> |
| D&R [19] | 77.99 | 77.37 |
| Ours | 79.51 | 79.37 |

TABLE VI
PERFORMANCE OF EACH MODALITY OF DIFFERENT METHODS ON CREMA-D AND KINETICS SOUNDS.

| Method | CREMA-D | | Kinetics-Sounds | |
|-------------------|--------------|--------------|-----------------|--------------|
| | Audio | Visual | Audio | Visual |
| Unimodal-training | 63.17 | 68.15 | 60.44 | 37.78 |
| Joint-training | 58.72 | 66.59 | 58.61 | 30.42 |
| OGM-GE [14] | 60.32 | 65.73 | 55.83 | 34.55 |
| PMR [18] | 59.02 | 67.83 | 57.63 | 33.14 |
| MLA [33] | 61.26 | 67.49 | 57.84 | 34.31 |
| Ours | <u>63.03</u> | 69.21 | 63.16 | <u>37.27</u> |

gains for all three optimizers. These findings confirm that our method is compatible with diverse optimizers and consistently enhances multimodal training.

3) *Comparison on Transformer-based Backbone*: In multi-modal learning, beyond convolution-based deep networks such as ResNet, more sophisticated transformer-based backbones are also widely adopted. Accordingly, we further conduct experiments with transformer-based backbones to compare various balanced multimodal learning methods. Following previous work [19], we employ the transformer encoder as the backbone of each unimodal encoder on the CMU-MOSI dataset, with model trained from scratch. Specifically, we use a 3-layer transformer encoder [66], where each layer (comprising multi-head self-attention and feed-forward parameters) is treated as a network block in our method. The results in Table V demonstrate that balanced multimodal learning methods are generally less effective on transformer-based backbones, which is consistent with previous findings [19]. Nevertheless, our method achieves superior performance compared to others, highlighting its stronger versatility.

E. Enhanced Unimodal Performance with AIM

As discussed in Sec. I and III-D, **AIM** can stimulate the learning of weak modalities without hindering the learning of the dominant modality, thereby improving balanced multimodal learning. To verify this, we observe the performance changes of each unimodal during **AIM** training and compare them with those under unimodal training, multimodal joint training, and the state-of-the-art **D&R** [19]. Fig. 4 presents the results for the audio and visual modalities on Kinetics-

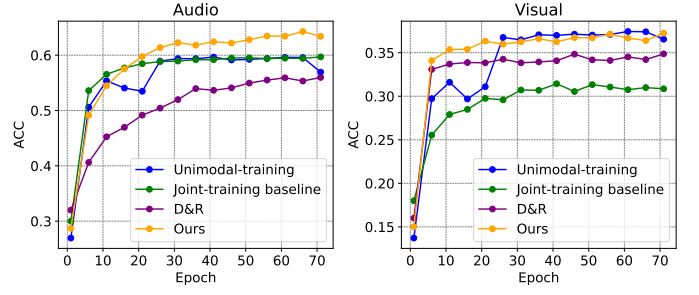


Fig. 4. Performance variation of two modalities on Kinetics-Sounds of different methods during training.

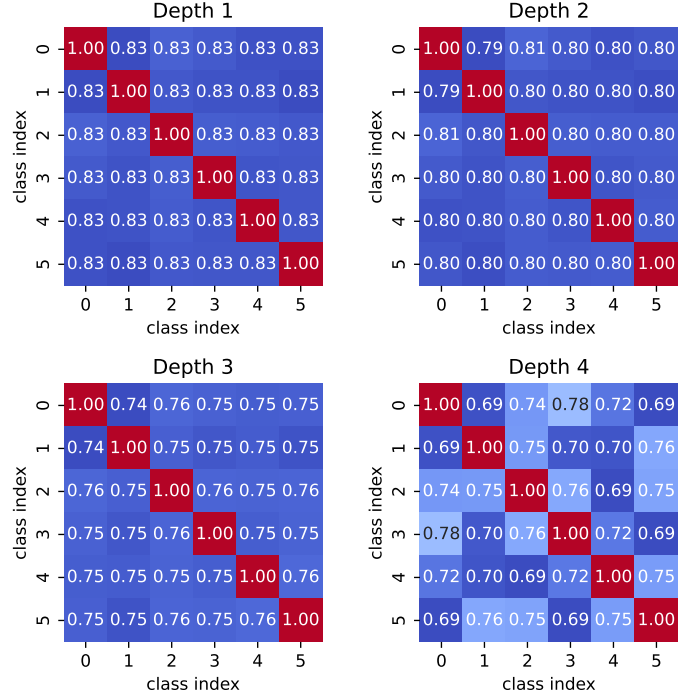


Fig. 5. Visualization of inter-class orthogonality of depth-adaptive prototypes at different depths on CREMA-D.

Sounds. The blue curves correspond to unimodal training, the green curves to joint training, the purple curves to **D&R**, and the orange curves to our proposed **AIM**.

From the results, the audio modality converges to a higher accuracy than the visual modality on Kinetics-Sounds, indicating that audio serves as the dominant modality. A comparison between the green and blue curves shows that the performance of the dominant audio modality remains similar under both unimodal and joint training, whereas the performance of the weaker visual modality drops substantially under joint training. This suggests that, during joint training, the dominant audio modality suppresses the learning of the weaker visual modality, resulting in an imbalanced learning outcome. The purple curve shows that **D&R** achieves better performance on the weak visual modality compared to joint training, but performs worse on the dominant audio modality than both unimodal training and joint training. This indicates that, although **D&R** effectively alleviates the suppression of the weak modality, it also hinders the learning of the dominant modality to some

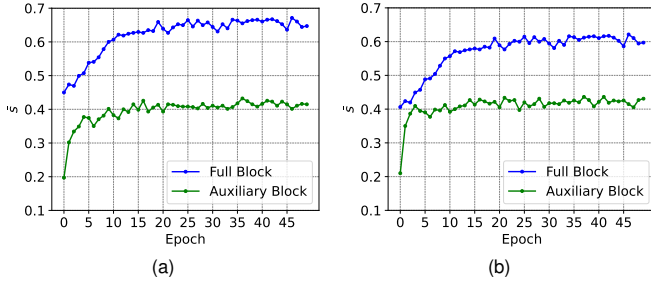


Fig. 6. Variation of the average performance \bar{s} of the dominant visual modality's full block and auxiliary block during training on CREMA-D.

TABLE VII
PERFORMANCE OF “**AIM-label**” AND **AIM** ON DIFFERENT DATASETS.

| Method | CREMA-D | | Kinetics-Sounds | |
|------------------|--------------|--------------|-----------------|--------------|
| | ACC | Macro-F1 | ACC | Macro-F1 |
| Joint-training | 67.47 | 67.80 | 65.04 | 65.12 |
| AIM-label | 80.11 | 80.24 | 71.05 | 70.82 |
| AIM | 81.32 | 82.00 | 72.40 | 72.27 |

extent. In contrast, the proposed **AIM** attains performance on the dominant audio modality comparable to unimodal training, while preserving the performance of the weak visual modality with negligible degradation. This demonstrates that **AIM** not only further alleviates the suppression of the weak modality but also retains the full potential of the dominant modality, thereby enhancing overall multimodal learning performance.

Table VI also compares the performance of each unimodal of some other representative balanced multimodal learning methods. It can be observed that although existing methods generally improve the performance of the weak modality compared to joint training, they often compromise the performance of the dominant modality. For example, on the CREMA-D dataset, they yield better audio performance than joint training but slightly worse visual performance. The proposed **AIM** outperforms joint training baseline on both modalities, achieving performance comparable to unimodal training. This indicates that **AIM** effectively enables learning without suppressing either the dominant modality or the weak modality.

F. Discussion on the Depth-Aware Prototypes

Depth-aware prototypes (**DAP**) are introduced in **AIM** to provide adaptive objectives at different network depths. To verify the improvement of **DAP** over using ground-truth labels for computing losses and assessing the optimization state at different depths, we introduce a variant “**AIM-label**” for comparison in our experiments. “**AIM-label**” employs the classifier to obtain the output class distribution of each modality at different depths, replacing the computation in Eq. (8) with the probability of the ground-truth class under the class distribution, and replacing Eq. (9) with the cross-entropy loss between the output class distribution and the labels. The comparison results between **AIM** and “**AIM-label**” in Table VII show that both “**AIM-label**” and **AIM** significantly improve multimodal performance compared to

TABLE VIII
ACCURACY OF **AIM** WITH DIFFERENT METRICS TO MEASURE THE PERFORMANCE DISCREPANCY BETWEEN MODALITIES IN EQ. (12).

| Dataset | CREMA-D | Kinetics-Sounds | UCF-101 |
|---------------------------------|--------------|-----------------|--------------|
| CV | 81.32 | 72.40 | 77.43 |
| MAD | 81.11 | 72.23 | 77.15 |
| Variance (σ^2) | 80.46 | 70.94 | 77.21 |
| Standard Deviation (σ) | 81.24 | 71.84 | 77.30 |

joint training, indicating their ability to address the imbalanced multimodal learning problem. **AIM** with **DAP** achieves a greater improvement than “**AIM-label**”, suggesting that the use of **DAP** supports more effective modulation in **AIM**.

To further evaluate the adaptivity of **DAP** to the optimization capacities at different depths, we compute the average orthogonality between class prototypes within each depth, as formulated in Eq. (14).

$$\mathcal{O}_d^m = \frac{1}{K(K-1)} \sum_{k_1=1}^K \sum_{k_2 \neq k_1}^K \cos[(p_d^m)_{k_1}, (p_d^m)_{k_2}], \quad (14)$$

where $\cos[\cdot, \cdot]$ is the cosine similarity, $(p_d^m)_k$ denotes the prototype of the k -th class at depth d for modality m . Fig. 5 presents the variation in average orthogonality of **DAP** across different depths d for the two modalities in CREMA-D. It can be observed that the orthogonality between prototypes increases with depth, indicating progressively stricter optimization objective. This demonstrates that **DAP** effectively adapts to the increasing optimization capacity of deeper layers, providing more suitable objectives for loss computation and optimization state evaluation at each depth.

G. Discussion on the Parameter-Adaptive Modulation

To investigate the effectiveness of the parameter decoupling module and the joint training of weak and pseudo-weak modalities in enhancing multimodal performance, we report the performance variations of the full network block of the dominant modality, the pseudo-weak modality block, the well-optimized parameter block, and the weak modality block under the proposed joint training strategy. The performance is evaluated using the method described in Eq. (8). For comparison, we also include the performance variations of the dominant and weak modalities under existing methods that directly suppress the dominant modality.

As shown in Fig. 6a, the performance of the pseudo-weak modality block is lower than that of the full network block for the dominant modality, while the well-optimized parameter block consistently achieves higher performance than the full network. This demonstrates that the parameter decoupling module effectively separates the network into well-optimized and under-optimized components.

Compared to direct suppression-based methods, our joint training of weak and pseudo-weak modalities not only improves the performance of the weak modality but also preserves or enhances the performance of the dominant modality. Furthermore, we isolate the pseudo-weak audio modality (as

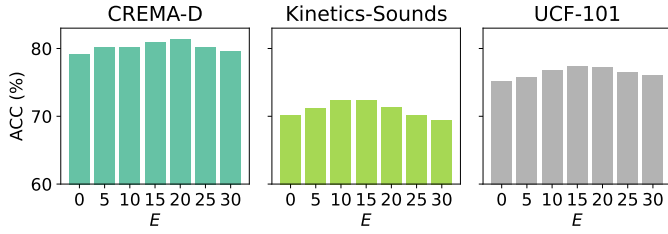


Fig. 7. Parameter analysis of E on different datasets.

dominant) and the weak visual modality for interaction. As shown in Fig. 6b, the performance of the dominant audio modality still surpasses that of methods that directly suppress it. This confirms that optimizing the pseudo-weak modality block positively influences the full dominant network block and highlights the dominant role of the pseudo-weak modality in enhancing its corresponding dominant modality.

H. Discussion on the Depth-Adaptive Modulation

In depth-adaptive modulation, the Coefficient of Variation (CV) is employed to quantify the performance disparity between modalities at each depth, thereby evaluating the imbalance level α_d , as defined in Eq. (12). Additional experiments were conducted to investigate the impact of different performance disparity measures on the model's results. We introduce three commonly used metrics, namely Mean Absolute Deviation (MAD), Variance (σ^2), and Standard Deviation (σ), whose computation formulas are given in $MAD = \frac{1}{M} \sum_{m=1}^M |s_d^m - \bar{s}_d|$, $\sigma^2 = \frac{1}{M} \sum_{m=1}^M (s_d^m - \bar{s}_d)^2$, and $\sigma = \sqrt{\sigma^2}$, respectively. s_d^m and \bar{s}_d are defined in Sec. III-E. As shown in Table VIII, **AIM** delivers consistently similar performance across different metrics, with CV producing better results than the other methods. This can be attributed to the fact that CV accounts for performance differences across different depths, effectively serving as a normalization step. MAD and Standard Deviation outperform Variance, likely because the latter produces more extreme values, which can lead to greater perturbations in modulation.

In addition, we compare the variation of modality performance discrepancy calculated via Eq. (12) across different training depths before and after applying our method. As shown in Fig. 1a, in the baseline without our method, the discrepancies at most depths fail to converge to a low level, reflecting substantial modality imbalance. In contrast, Fig. 1b demonstrates that with our method, the learning at each depth is adaptively modulated according to its imbalance level, leading to consistently lower discrepancies across depths.

I. Parameter Analysis

In the multimodal joint training framework incorporating **AIM**, there is a hyperparameter E that specifies the number of epochs the multimodal framework is trained before **AIM** is introduced, as illustrated in Algorithm 1. Additional experiments are conducted to investigate the impact of E on the training results. Fig. 7 presents the results for different values of E , where $E = 0$ indicates that **AIM** is applied from the beginning

of training. As E increases, the multimodal performance after training first shows a slight improvement and then declines, remaining relatively stable overall. This trend can be explained as follows: when **AIM** is introduced too early (small E), the multimodal framework is not yet well trained, leading to suboptimal depth-aware prototypes and thus less effective modulation in the early stages of training. Conversely, when **AIM** is introduced too late (large E), modality imbalance issues within the multimodal framework are not addressed promptly, resulting in suboptimal training performance.

V. CONCLUSIONS

This paper highlights a previously overlooked issue in previous works termed intra-network optimization bias and proposes Adaptive Intra-Network Modulation (**AIM**), which enables adaptive modulation of the learning of different parameters and depths within a multimodal network. On one hand, **AIM** introduces a novel parameter decoupling mechanism and an auxiliary-weak interaction mechanism that enhances the learning of under-trained parameters of the dominant modality while avoiding the suppression of weaker modalities, thereby enabling efficient learning for all modalities. On the other hand, **AIM** adapts to the varying levels of modality imbalance caused by convergence bias at different depths, further improving the effectiveness of balanced multimodal modulation. In addition, depth-aware prototypes (**DAP**) are introduced to account for the optimization capacity of networks at different depths, providing depth-adaptive performance evaluation and loss computation objectives for **AIM**. Extensive experiments on multiple datasets spanning diverse modality types and tasks demonstrate that **AIM** achieves superior multimodal and unimodal performance compared with state-of-the-art methods for balanced multimodal learning. Further experiments with different fusion strategies, optimizers, and backbone encoders verify the versatility and generality of **AIM**. Ablation studies and in-depth analyses further confirm the contributions of intra-network parameter-adaptive modulation and depth-adaptive modulation to balanced multimodal learning, as well as the effectiveness of each component.

Although current balanced multimodal learning methods have shown great effectiveness on classification tasks, they lack thorough investigation for regression tasks. This reveals an important open problem. Accordingly, in future work, we will further extend **AIM** to a broader range of machine learning tasks including regression.

REFERENCES

- [1] M. S. Gazzaniga, R. B. Ivry, and G. Mangun, "Cognitive neuroscience. the biology of the mind,(2014)," 2006.
- [2] E. B. Herreras, "Cognitive neuroscience; the biology of the mind," *Cuadernos de Neuropsicología/Panamerican Journal of Neuropsychology*, vol. 4, no. 1, pp. 87–90, 2010.
- [3] N. Srivastava and R. R. Salakhutdinov, "Multimodal learning with deep boltzmann machines," *Advances in neural information processing systems*, vol. 25, 2012.
- [4] S. K. Shankar, L. P. Prieto, M. J. Rodríguez-Triana, and A. Ruiz-Calleja, "A review of multimodal learning analytics architectures," in *2018 IEEE 18th international conference on advanced learning technologies (ICALT)*. IEEE, 2018, pp. 212–214.
- [5] J. Ngiam, A. Khosla, M. Kim, J. Nam, H. Lee, A. Y. Ng *et al.*, "Multimodal deep learning," in *ICML*, vol. 11, 2011, pp. 689–696.

- [6] P. P. Liang, A. Zadeh, and L.-P. Morency, "Foundations and trends in multimodal machine learning: Principles, challenges, and open questions," *arXiv preprint arXiv:2209.03430*, 2022.
- [7] T. Baltrušaitis, C. Ahuja, and L.-P. Morency, "Multimodal machine learning: A survey and taxonomy," *IEEE transactions on pattern analysis and machine intelligence*, vol. 41, no. 2, pp. 423–443, 2018.
- [8] E. Kazakos, A. Nagrani, A. Zisserman, and D. Damen, "Epic-fusion: Audio-visual temporal binding for egocentric action recognition," in *Proceedings of the IEEE/CVF international conference on computer vision*, 2019, pp. 5492–5501.
- [9] R. Gao, T.-H. Oh, K. Grauman, and L. Torresani, "Listen to look: Action recognition by previewing audio," in *Proceedings of the IEEE/CVF conference on computer vision and pattern recognition*, 2020, pp. 10457–10467.
- [10] D. Hazarika, R. Zimmermann, and S. Poria, "Misa: Modality-invariant and-specific representations for multimodal sentiment analysis," in *Proceedings of the 28th ACM international conference on multimedia*, 2020, pp. 1122–1131.
- [11] H. Sun, H. Wang, J. Liu, Y.-W. Chen, and L. Lin, "Cubemlp: An mlp-based model for multimodal sentiment analysis and depression estimation," in *Proceedings of the 30th ACM international conference on multimedia*, 2022, pp. 3722–3729.
- [12] G. Potamianos, C. Nefi, J. Luettin, and I. Matthews, "Audio-visual automatic speech recognition: An overview," *Issues in visual and audio-visual speech processing*, vol. 22, p. 23, 2004.
- [13] Y. Huang, J. Lin, C. Zhou, H. Yang, and L. Huang, "Modality competition: What makes joint training of multi-modal network fail in deep learning?(provably)," in *International conference on machine learning*. PMLR, 2022, pp. 9226–9259.
- [14] X. Peng, Y. Wei, A. Deng, D. Wang, and D. Hu, "Balanced multimodal learning via on-the-fly gradient modulation," in *Proceedings of the IEEE/CVF conference on computer vision and pattern recognition*, 2022, pp. 8238–8247.
- [15] W. Wang, D. Tran, and M. Feiszli, "What makes training multi-modal classification networks hard?" in *Proceedings of the IEEE/CVF conference on computer vision and pattern recognition*, 2020, pp. 12695–12705.
- [16] Y. Wei, D. Hu, H. Du, and J.-R. Wen, "On-the-fly modulation for balanced multimodal learning," *IEEE Transactions on Pattern Analysis and Machine Intelligence*, 2024.
- [17] N. Wu, S. Jastrzebski, K. Cho, and K. J. Geras, "Characterizing and overcoming the greedy nature of learning in multi-modal deep neural networks," in *International Conference on Machine Learning*. PMLR, 2022, pp. 24043–24055.
- [18] Y. Fan, W. Xu, H. Wang, J. Wang, and S. Guo, "Pmr: Prototypical modal rebalance for multimodal learning," in *Proceedings of the IEEE/CVF Conference on Computer Vision and Pattern Recognition*, 2023, pp. 20029–20038.
- [19] Y. Wei, S. Li, R. Feng, and D. Hu, "Diagnosing and re-learning for balanced multimodal learning," in *European Conference on Computer Vision*. Springer, 2024, pp. 71–86.
- [20] H. Saratchandran, S. Ramasinghe, and S. Lucey, "From activation to initialization: Scaling insights for optimizing neural fields," in *Proceedings of the IEEE/CVF Conference on Computer Vision and Pattern Recognition*, 2024, pp. 413–422.
- [21] Y. Chen, A. Yuille, and Z. Zhou, "Which layer is learning faster? a systematic exploration of layer-wise convergence rate for deep neural networks," in *The Eleventh International Conference on Learning Representations*, 2023.
- [22] L. Liu, X. Cao, H. Wang, and J. Xiang, "Optimization of model parameters and hyperparameters in deep learning models for spatial interaction prediction," *Expert Systems with Applications*, vol. 266, p. 126160, 2025.
- [23] D. Ramachandram and G. W. Taylor, "Deep multimodal learning: A survey on recent advances and trends," *IEEE signal processing magazine*, vol. 34, no. 6, pp. 96–108, 2017.
- [24] Y. Zhu, Y. Wu, N. Sebe, and Y. Yan, "Vision+ x: A survey on multimodal learning in the light of data," *IEEE Transactions on Pattern Analysis and Machine Intelligence*, 2024.
- [25] S. Li, T. Zhang, B. Chen, and C. L. P. Chen, "Mia-net: Multi-modal interactive attention network for multi-modal affective analysis," *IEEE Transactions on Affective Computing*, vol. 14, no. 4, pp. 2796–2809, 2023.
- [26] T. Zhang, S. Li, B. Chen, H. Yuan, and C. L. Philip Chen, "Aia-net: Adaptive interactive attention network for text-audio emotion recognition," *IEEE Transactions on Cybernetics*, vol. 53, no. 12, pp. 7659–7671, Dec 2023.
- [27] S. Li, T. Zhang, and C. L. P. Chen, "Sia-net: Sparse interactive attention network for multimodal emotion recognition," *IEEE Transactions on Computational Social Systems*, vol. 11, no. 5, pp. 6782–6794, 2024.
- [28] —, "Cyclic data distillation semi-supervised learning for multi-modal emotion recognition," *IEEE Transactions on Knowledge and Data Engineering*, pp. 1–14, 2025.
- [29] D. Hu, X. Li *et al.*, "Temporal multimodal learning in audiovisual speech recognition," in *Proceedings of the IEEE Conference on Computer Vision and Pattern Recognition*, 2016, pp. 3574–3582.
- [30] H. Yu, J. Tang, G. Wang, and X. Gao, "A novel multi-view clustering method for unknown mapping relationships between cross-view samples," in *Proceedings of the 27th ACM SIGKDD conference on knowledge discovery & data mining*, 2021, pp. 2075–2083.
- [31] M. Yang, Y. Li, P. Hu, J. Bai, J. Lv, and X. Peng, "Robust multi-view clustering with incomplete information," *IEEE Transactions on Pattern Analysis and Machine Intelligence*, vol. 45, no. 1, pp. 1055–1069, 2022.
- [32] P. Zeng, M. Yang, Y. Lu, C. Zhang, P. Hu, and X. Peng, "Semantic invariant multi-view clustering with fully incomplete information," *IEEE Transactions on Pattern Analysis and Machine Intelligence*, vol. 46, no. 4, pp. 2139–2150, 2023.
- [33] X. Zhang, J. Yoon, M. Bansal, and H. Yao, "Multimodal representation learning by alternating unimodal adaptation," in *Proceedings of the IEEE/CVF conference on computer vision and pattern recognition*, 2024, pp. 27456–27466.
- [34] Q. Zhang, H. Wu, C. Zhang, Q. Hu, H. Fu, J. T. Zhou, and X. Peng, "Provable dynamic fusion for low-quality multimodal data," in *International conference on machine learning*. PMLR, 2023, pp. 41753–41769.
- [35] B. Cao, Y. Xia, Y. Ding, C. Zhang, and Q. Hu, "Predictive dynamic fusion," in *Proceedings of the 41st International Conference on Machine Learning*, ser. Proceedings of Machine Learning Research, R. Salakhutdinov, Z. Kolter, K. Heller, A. Weller, N. Oliver, J. Scarlett, and F. Berkenkamp, Eds., vol. 235. PMLR, 21–27 Jul 2024, pp. 5608–5628. [Online]. Available: <https://proceedings.mlr.press/v235/cao24c.html>
- [36] Y. Sun, S. Mai, and H. Hu, "Learning to balance the learning rates between various modalities via adaptive tracking factor," *IEEE Signal Processing Letters*, vol. 28, pp. 1650–1654, 2021.
- [37] C. Du, T. Li, Y. Liu, Z. Wen, T. Hua, Y. Wang, and H. Zhao, "Improving multi-modal learning with uni-modal teachers," *arXiv preprint arXiv:2106.11059*, 2021.
- [38] M. A. Nielsen, *Neural networks and deep learning*. Determination press San Francisco, CA, USA, 2015, vol. 25.
- [39] T. Li, M. Xu, Z. Liu, Y. Chen, and K. Li, "A deep transformer-based fast cu partition approach for inter-mode vvc," *IEEE Transactions on Image Processing*, vol. 34, pp. 1133–1148, 2025.
- [40] S. Hochreiter, "Untersuchungen zu dynamischen neuronalen netzen," *Diploma, Technische Universität München*, vol. 91, no. 1, p. 31, 1991.
- [41] S. Hochreiter, Y. Bengio, P. Frasconi, J. Schmidhuber *et al.*, "Gradient flow in recurrent nets: the difficulty of learning long-term dependencies," 2001.
- [42] G. Huang, Y. Sun, Z. Liu, D. Sedra, and K. Q. Weinberger, "Deep networks with stochastic depth," in *European conference on computer vision*. Springer, 2016, pp. 646–661.
- [43] A. Brock, T. Lim, J. M. Ritchie, and N. Weston, "Freezeout: Accelerate training by progressively freezing layers," *arXiv preprint arXiv:1706.04983*, 2017.
- [44] V. V. Ramasesh, E. Dyer, and M. Raghu, "Anatomy of catastrophic forgetting: Hidden representations and task semantics," *arXiv preprint arXiv:2007.07400*, 2020.
- [45] J. Snell, K. Swersky, and R. Zemel, "Prototypical networks for few-shot learning," *Advances in neural information processing systems*, vol. 30, 2017.
- [46] V. Roy, Y. Xu, Y.-X. Wang, K. Kitani, R. Salakhutdinov, and M. Hebert, "Few-shot learning with intra-class knowledge transfer," *arXiv preprint arXiv:2008.09892*, 2020.
- [47] T. Gao, X. Han, Z. Liu, and M. Sun, "Hybrid attention-based prototypical networks for noisy few-shot relation classification," in *Proceedings of the AAAI conference on artificial intelligence*, vol. 33, no. 01, 2019, pp. 6407–6414.
- [48] K. Ding, J. Wang, J. Li, K. Shu, C. Liu, and H. Liu, "Graph prototypical networks for few-shot learning on attributed networks," in *Proceedings of the 29th ACM international conference on information & knowledge management*, 2020, pp. 295–304.
- [49] S. Seifi, D. O. Reino, N. Chumerin, and R. Aljundi, "Ood aware supervised contrastive learning," in *Proceedings of the IEEE/CVF Winter Conference on Applications of Computer Vision*, 2024, pp. 1956–1966.

- [50] Y. Yang, H. Wang, and D. Katabi, "On multi-domain long-tailed recognition, imbalanced domain generalization and beyond," in *European conference on computer vision*. Springer, 2022, pp. 57–75.
- [51] Y. Pan, T. Yao, Y. Li, Y. Wang, C.-W. Ngo, and T. Mei, "Transferrable prototypical networks for unsupervised domain adaptation," in *Proceedings of the IEEE/CVF conference on computer vision and pattern recognition*, 2019, pp. 2239–2247.
- [52] Y. Chai, L. Du, J. Qiu, L. Yin, and Z. Tian, "Dynamic prototype network based on sample adaptation for few-shot malware detection," *IEEE Transactions on Knowledge and Data Engineering*, vol. 35, no. 5, pp. 4754–4766, 2022.
- [53] J. Li, P. Zhou, C. Xiong, and S. C. Hoi, "Prototypical contrastive learning of unsupervised representations," *arXiv preprint arXiv:2005.04966*, 2020.
- [54] H. Abdi, "Coefficient of variation," *Encyclopedia of research design*, vol. 1, no. 5, pp. 169–171, 2010.
- [55] H. Cao, D. G. Cooper, M. K. Keutmann, R. C. Gur, A. Nenkov, and R. Verma, "Crema-d: Crowd-sourced emotional multimodal actors dataset," *IEEE transactions on affective computing*, vol. 5, no. 4, pp. 377–390, 2014.
- [56] R. Arandjelovic and A. Zisserman, "Look, listen and learn," in *Proceedings of the IEEE international conference on computer vision*, 2017, pp. 609–617.
- [57] W. Kay, J. Carreira, K. Simonyan, B. Zhang, C. Hillier, S. Vijayanarasimhan, F. Viola, T. Green, T. Back, P. Natsev *et al.*, "The kinetics human action video dataset," *arXiv preprint arXiv:1705.06950*, 2017.
- [58] K. Soomro, A. R. Zamir, and M. Shah, "Ucf101: A dataset of 101 human actions classes from videos in the wild," *arXiv preprint arXiv:1212.0402*, 2012.
- [59] A. Zadeh, R. Zellers, E. Pincus, and L.-P. Morency, "Mosi: multimodal corpus of sentiment intensity and subjectivity analysis in online opinion videos," *arXiv preprint arXiv:1606.06259*, 2016.
- [60] H. Li, X. Li, P. Hu, Y. Lei, C. Li, and Y. Zhou, "Boosting multi-modal model performance with adaptive gradient modulation," in *Proceedings of the IEEE/CVF International Conference on Computer Vision*, 2023, pp. 22 214–22 224.
- [61] D. Kiela, E. Grave, A. Joulin, and T. Mikolov, "Efficient large-scale multi-modal classification," in *Proceedings of the AAAI conference on artificial intelligence*, vol. 32, no. 1, 2018.
- [62] E. Perez, F. Strub, H. De Vries, V. Dumoulin, and A. Courville, "Film: Visual reasoning with a general conditioning layer," in *Proceedings of the AAAI conference on artificial intelligence*, vol. 32, no. 1, 2018.
- [63] A. Owens and A. A. Efros, "Audio-visual scene analysis with self-supervised multisensory features," in *Proceedings of the European conference on computer vision (ECCV)*, 2018, pp. 631–648.
- [64] K. D. B. J. Adam *et al.*, "A method for stochastic optimization," *arXiv preprint arXiv:1412.6980*, vol. 1412, no. 6, 2014.
- [65] J. Duchi, E. Hazan, and Y. Singer, "Adaptive subgradient methods for online learning and stochastic optimization," *Journal of machine learning research*, vol. 12, no. 7, 2011.
- [66] P. P. Liang, Y. Lyu, X. Fan, Z. Wu, Y. Cheng, J. Wu, L. Chen, P. Wu, M. A. Lee, Y. Zhu *et al.*, "Multibench: Multiscale benchmarks for multimodal representation learning," *Advances in neural information processing systems*, vol. 2021, no. DB1, p. 1, 2021.